Fluid Flow, Inclusion removal and Slag Entrapment in Molten Steel Continuous Casting Mould

Abdelbagi Mohamed Abdalla#1, Omar Ahmad Althami #2
Mechanical Engineering Department, University of Kordofan, Sudan#1
#Mechanical Engineering Department, University of Karary, Sudan#2

ABSTRACT

The research of "Investigation to improve the secondary steel manufacturing process by adopting mathematical models" was considered to contribute to the Strategic Steel Research in Sudan. The project was suggested as a close collaboration between Department of mechanical engineering-University of Karrary and the steel factories in Sudan.

Steel cleanliness, which is aim of this project, is a focal point for Sudan young steel industry in order to maintain and strengthen their in-market and global competitiveness.The steady velocity fields were obtained by computationally solving, the Reynolds-Averaged Navier-Strokes (RANS) equations using the standard k-ε and k-ω models of turbulence. These flow fields are then implemented to predict the inclusion removal by solving the inclusion transport equationnumerically.The Volume of Fluid(VOF) method was employed to model the behavior of the interfaces of the liquid steel – liquid slag – air system (to evaluate slag entrapment.) usinga two-dimensional, transient solution. The calculations were carried out using the commercial Computational Fluid Dynamics (CFD) software ANSYS-FLUENT 6.3.26.

The models results were compared and validated with experiments results, plant measurements and models reported in the open literature.

The predicted inclusion separation fractions to the top surface (slag) were compared and well agreed with the published data from [2] [3]. The computed results of the interface tracking between slag and steel had revealed that the "entrapment" of fine slag portions into liquid steel was occurred in the system of the present model configuration.

The project findings considered as first step and intended to be hopefully applied in the steel factories in Sudan.

Key words: *Steel cleanliness; SEN-CC Mold; Turbulent flow; Slag entrapment; Inclusion separation; Model validation; CFD.*

I.INTRODUCTION

Conventional continuous casting is one of the most cost effective production routes for producing semi-finished materials from molten steel. This cost–effectiveness is largely dependent on both quantity and quality of the final products. Therefore, it is important to control the dependent physical phenomena occurring at the same time inside the mould such as heat transfer, solidification and fluid flow to offer a steady and smooth casting process. This then decreases the probability of defects (i.e, transverse and longitudinal cracks,deep wavy marks etc.) and increases the overall production in the form of reducedrequisite for surface treatments and a decreased amount of scrapped materials [28]

The first objective of this sub-model within this research was to develop a mathematical model of the flow pattern in the liquid pool which determines how both molten steel and inclusion particles carried in by the nozzle are distributed. To verify acceptable accuracy of the model, its predictions were compared with experiments and models conducted by [2] [3].

This work represents the first step in the development of comprehensive system of mathematical models of fluid flow,slag entrapment and heat transfer, within the continuous slab-casting mold, which will ultimately be applied to predict and understand the effects of such diverse variables, but now only fluid flow pattern, which is essential for the modeling of other variables, slag entrapment and inclusion separation fraction were considered. Due to [2],quality control observations in a steel plant have indicated many severe quality problems, including inclusion entrapment, are directly related to the flow pattern in the mold.

Plant observations and final products mechanical properties tests in GIAD steel factory in Sudan have found that a serious quality problems, mainly brittleness of the final product (building bars), which may be as the results of many factors, including inclusion entrapment, slag entrapment in the steel melt and flow pattern in the mold.

As the results, these problems affect the productivity as well the improvement of the final product quality, which are permanent requirements concerning the continuous casting process, this was the motivation signal to conduct this research.
Thus optimization and control of the fluid flow pattern in the continuous casting mold to remove inclusions prevent slag entrainment is quite necessary to the steel industry.Some variables like the nozzle and mold geometry, steel flow rate,submergence depth, flux layer properties andargon injection rate can control the flow pattern in the mold. The nozzle play asignificantrole for controlling flow pattern in mold, therefore, by using various designs of the nozzle, it would be an easy and low-cost way to improve the fluid flow in the mold[2] [5]. The fluid flow in the continuous casting mold can be inspected by physical modeling,industrial trials or mathematical modeling[2] [3].
In the last decades mathematical modeling became an effective, economical tool to become information that cannot be directly measured in the steel melt.
Sometimes the facilities to carry out experimental work may not (yet) available, in such case the CFD user must depend on among other on comparisons with high-quality data from closely related problems documented in the literature [1]. Therefore the validation and verification of the present models are carried out using results from experimental and modeling results from other researchers.
A3-D, steady flow of steel in the liquid pool in the mold is simulated with finite-volume based software (ANSYS_FLUENT), the turbulence models implemented are the standard k-ε as well as k-ω. Inclusion trajectories are computed by integrating each local velocity, considering its buoyancy and drag forces. The effect of turbulent fluctuations on the particle motion is incorporated by the "random walk" model [12].
The full trajectory calculations solve a transport equation for each particle as it travels through the calculated fluid flow velocity field. The present models was based onthe models and plant measurement from [2] [3][7].
The volume of fluid (VOF) free surface model is a simplification of the mixture model and has been successfully applied in predicting and modeling the continuous casting mold [4] [7] [8] [9] [10] [11]. The VOF model can simulate two or more immiscible fluid phases, in which the position of the interface between the fluids is of interest. This model was implemented in this work, to evaluate slag entrapment in the steel melt.

II. Pre-processing: geometry and grid generation

Symmetry assumed:

In the present work, symmetrical flow is presumed. Therefore Fig. 1 depicts a 3D and 2D half model of the tundish, which is also indicating boundary conditions.

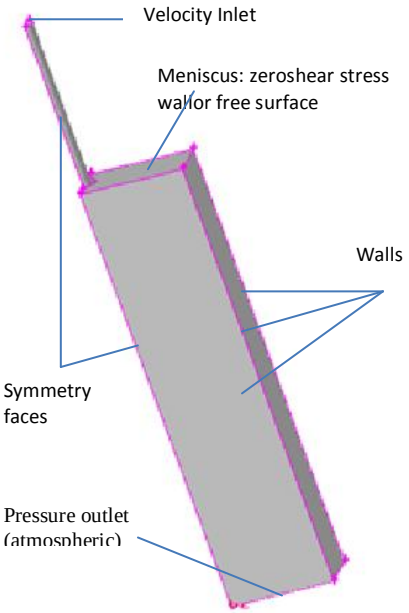

Fig.13D half model without the mesh to indicate boundary conditions.

For any CFD flow problem to be solved, Pre-processing is needed, to comprise the preparation of the geometry as well as dividing the domain of the flow into cells (grid) fig 2. Pre-processing can be described as process of geometry and initial generation of the grid.

Pre-processing generates and initialize grid before the CFD solution process is commenced and taking place. Most CFD codes consist of an option to alter the grid based on the solution in progress, also recognized as solution adaptive-gridding. These grid refinement or coarsening, occur during the solution procedure and are clearly not part of pre-processing in CFD models. The pre-processor used in the present research is ANSYS-GAMBIT 2.4, which is the pre-processor for ANSYS-FLUENT [16].

A 2D as well as 3D half model geometry and mesh were constructed using approximately 422470 quadrilateral and 985232 tetrahedral cells respectively, using the pre-processor GAMBIT (Fig. 2) and then exported the mesh to FLUENT to set up all CFD parameters

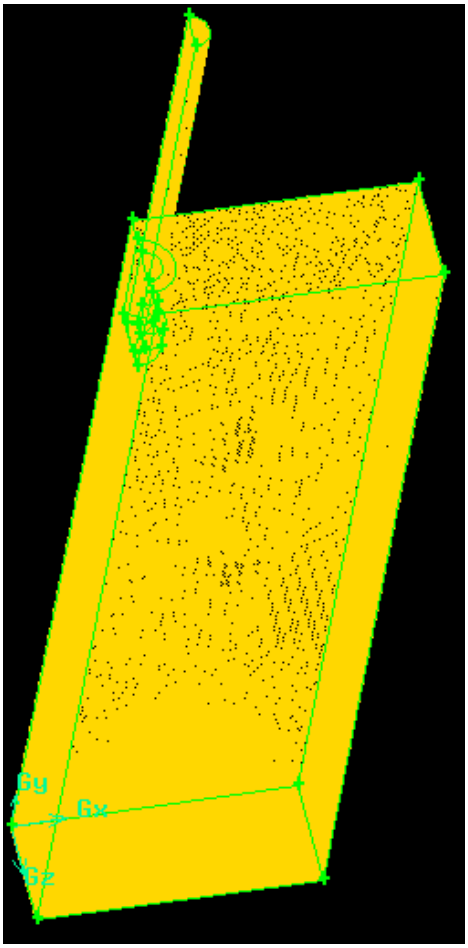

Fig.2The mesh or grid of the 3D combined SEN and the half mold.

In the present work, the submerged entry nozzle(SEN) and mold will be simulated together (combined) in one CFD model for better correspondence with plant circumstances (see Fig.3 below). This complicates the flow field, especially at the nozzle ports as the flow exits into the mold cavity.

When separating the SEN from the mold (this is the case in the majority of the simulations of the SEN and the mold in the open literature), solutions seem to be more stable and converge quickly to predetermine criteria [25]. However, when assessing the SEN separately, a pressure outlet boundary condition is implemented to the SEN where it exits into the mold cavity. The pressure will typically be assumed to be the ferrostatic pressure due to the submergence depth of the SEN below the meniscus. The fluid flow in the SEN is then computed and the velocity profile of the SEN exit nozzle is appliedin a separate simulation to the mould as a velocity inlet boundary [25].

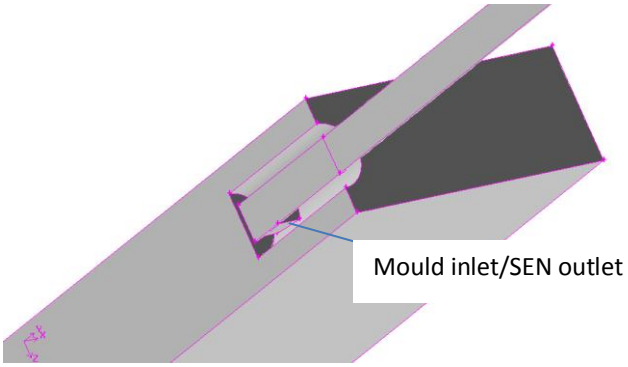

Fig.3 Illustrate the geometry details at the SEN and mold junction

III.The governing equations and Assumptions

A. Continuity equation, Navier-Stokes equations and k-ε&k-ω turbulence

In present work, incompressible steady flow in the mould cavity was simulated with 3-D as well as 2D finite-volume computational models using the k-ε and k-ω turbulence models in FLUENT.

Also incompressible steady as well as unsteady flow in the strand of the continuous caster is simulated with 2D model, using the realizable k-ε turbulence model.

The continuity equation and Navier-Stokes equations for the steady fluid flow ofincompressible Newtonian fluids are [13][2] [14]:

$$\frac{\partial}{\partial x_i}(\rho u_i) = 0,(1)$$

$$\frac{\partial}{\partial x_i}\left(\rho u_i u_j\right) = -\frac{\partial P}{\partial x_i} + (\mu_0 + \mu_t)\frac{\partial}{\partial x_j}\left(\frac{\partial u_i}{\partial x_j} + \frac{\partial u_j}{\partial x_i}\right) + \rho g_i + F_j (2)$$

Whereu_i, velocity component in xi direction (m/s); ρ, liquid density (kg/m^3); μ_t, turbulence viscosity (kg/m-s); P, pressure field (N/m^2); μ_o, laminar viscosity (kg/m-s); g_j, magnitude of gravity in j direction (m/s^2); ; i, j, are coordinate direction indices, which when reiterated in a term, denotes the summation of all three possible terms,F_j, other body forces. The turbulent viscosity for the k-ε Model [2], [13][15], is given by

$$\mu_t = \rho C_\mu \frac{k^2}{\varepsilon}(3)$$

Where ε= turbulent dissipation field, m^2/s^3, C_μ, empirical constant = 0.09; k, turbulent kinetic energy field, m^2/s^2 [6].For the transport of turbulent kinetic energy and kinetic energy dissipation rate, there are two additional partial differential equations given by [[2] [5]:

$$\rho u_j \frac{\partial k}{\partial x_j} = \frac{\partial}{\partial x_j}\left(\frac{\mu_t}{\sigma_K}\frac{\partial k}{\partial x_j}\right) + \mu_t \frac{\partial v_j}{\partial x_i}\left(\frac{\partial u_i}{\partial x_j} + \frac{\partial u_j}{\partial x_i}\right) - \rho\varepsilon \quad (4)$$

$$\rho v_j \frac{\partial \varepsilon}{\partial x_j} = \frac{\partial}{\partial x_j}\left(\frac{\mu_t}{\sigma_\varepsilon}\frac{\partial \varepsilon}{\partial x_j}\right) + C_1\,\mu_t \frac{\varepsilon}{K}\frac{\partial u_j}{\partial x_i}\left(\frac{\partial u_i}{\partial x_j} + \frac{\partial u_j}{\partial x_i}\right) - C_2 \frac{\varepsilon}{K}\rho\varepsilon \quad (5)$$

Where ∂/∂xi, differentiation with respect to coordinate direction x,y, or z (m); σ_K, σ_ε, empirical constants (1.0, 1.3); C_1, C_2, empirical constants (1.44, 1.92). The k-ε Model requests special "wall functions" as boundary conditions, in order to attain reasonable accuracy on a coarse grid [16].

The standard *k-ω* model is an empirical model based on model transport equations for the turbulence kinetic energy (*k*) and the specific dissipation rate (*ω*), which can also be thought of as the ratio of εto *k* [12]. As the *k-ω* model has been altered over the years, production terms have been added to both the *k* and *ω* equations, which have enhanced the correctness of the model for calculating free shear flows.

Transport Equations for the Standard k-ωModel

The turbulence kinetic energy, *k*, and the specific dissipation rate, *ω*, are obtained from the following transport equations:

$$\rho u_j \frac{\partial k}{\partial x_j} = \frac{\partial}{\partial x_j}\left(\Gamma_k \frac{\partial k}{\partial x_j}\right) + G_k - Y_k + S_k \quad (6)$$

$$\rho u_j \frac{\partial \omega}{\partial x_j} = \frac{\partial}{\partial x_j}\left(\Gamma_\omega \frac{\partial \omega}{\partial x_j}\right) + G_\omega - Y_\omega + S_\omega \quad (7)$$

Where, $G_k$symbolizes the generation of turbulence kinetic energy due to mean velocity gradients. G_ω represents the generation of ω. Y_k and Yωsymbolize the dissipation of k and ω due to turbulence, Γ_k and Γ_ω symbolize the effective diffusivity of k and ω, respectively. All of the above terms are calculated as described below. $S_k$and S_ω are user defined source terms[12].

Modeling the Effective Diffusivity

The effective diffusivities for the k-ω model are given by:

$$\Gamma_k = \mu + \frac{\mu_t}{\sigma_K} \quad (8)$$

$$\Gamma_\omega = \mu + \frac{\mu_t}{\sigma_\omega} \quad (9)$$

where$\sigma_k$and $\sigma_\omega$are the turbulent Prandtl numbers for *k* and *ω*, respectively.
The turbulent viscosity,μ_t, is computed by combining *k* and *ω*as follows:

$$\mu_t = \alpha^* \frac{\rho k}{\omega} \quad (10)$$

Note that α^* = 1 for high Reynolds number form of the *k-ω* model [12]

$$G_k = -\overline{\rho u'_i u'_j}\frac{\partial u_j}{\partial u_{x_i}} \quad (11)$$

$$G_\omega = \alpha \frac{\omega}{k} G_k \quad (12)$$

Note that $\alpha = \alpha_\infty$ = 1 for high Reynolds number form of the *k-ω* model

The dissipation of k is given by

$$Y_k = \rho\beta^* f_{\beta^*} k\omega \quad (13)$$

The dissipation of *ω* is given by

$$Y_\omega = \rho\beta f_\beta \omega^2 \quad (14)$$

B.Turbulence model:

A jet exiting into a larger cavity (such as the SEN nozzle exiting into the mould) definitely proposes turbulent flow [17]. FLUENT offers a number of viscous and turbulence models to suit most flow problem types. Whenever a turbulent flow situation is anticipated, the k-ε turbulence model is usually implemented because of its adequate accuracy (in most circumstances) as opposed to relative little computing time [29]. In this work Realizable k-ε for 2D-model and Standard k-ω for 3D model were used.

C.Inclusion removal in the continuous casting mold

The trajectory of every particle can be calculated incrementally by integrating its local velocity. The local velocity of inclusions is represented by Eq.(15) allowing for force balance between the drag force and the gravitational force [[18] [19][20].

$$\frac{du_{pi}}{dt} = \frac{3}{4}\frac{1}{d_p}\frac{\rho}{\rho_p} C_D\,(u_{pi} - u_i)^2 - \frac{(\rho - \rho_p)}{\rho_p} g_i \quad (15)$$

Where$u_{p,i}$, the particle velocity,ρ_p, ρ,the particle and liquid densities, kg/m^3; m/s; C_D, the drag coefficient as a function of particle Reynolds number, given as below [2], [21]

$$C_D = \frac{24}{Re_p}(1 + 0.186\ \mathrm{Re_p}^{0.653}) \quad (16)$$

To incorporate the effect of turbulent fluctuations on the particle motion,a "random walk" model is implemented. In which particle velocity fluctuations are based on a Gaussian-distributed

random number, selected according to the local turbulent kinetic energy. The random number is changed, thus generating a new instantaneous velocity fluctuation, at a frequency equal to the characteristic lifetime of the eddy. The instantaneous fluid velocity can be symbolized by [2] [21]:

$$U = \bar{u} + u' \quad (17)$$

$$u' = \xi \sqrt{\overline{u'^2}} = \xi \sqrt{\frac{2k}{3}} \quad (18)$$

Where u' is the instantaneous fluid velocity, m/s;$\bar{u}$ is the mean fluid phase velocity, m/s; u′ random velocity fluctuation, m/s; ξ the random number.

As boundary conditions for the particle motion, particles entrapped, when they touch wide faces and narrow faces which represent the dendritic solidification front and are escape at the top surface and the open bottom but are reflected at symmetry plane [2].

D. Slag, air and steel melt interface tracking (Volume of fluid method VOF)

The VOF [5] [22] model belongs to the Eularian type category and can be used for systems composed of two or more phase in the number of (q), e.g. for interface tracking between liquid slag-melting steel with a movable free surface.

In VOF method, the variable density equations of motion are solved for the mixture, and an extra transport equation for the volume fraction of each phase is solved, which can track the interface between the air, slag (flux) and the steel melt in the cc mold. The single momentum equation is solved throughout the domain, and the resulting velocity field is shared among the phases. This momentum equation, presented below, is dependent on the volume fractions of all phases through the properties ρ and μ[5] [22].

$$\frac{\partial(\rho v_i)}{\partial t} + \frac{\partial(\rho v_i v_j)}{\partial x_j} = \frac{\partial p}{\partial x_i} + \frac{\partial}{\partial x_j}\left[\mu\left(\frac{\partial v_i}{\partial x_j} + \frac{\partial v_j}{\partial x_i}\right)\right] + \rho g_i \quad (19)$$

Where ρ is the average density and can be calculated according to the density of q^{th} phase, which varies between 0 and 1, as,

$$\rho = \sum \alpha_q \rho_q \quad (20)$$

The transport equation for the volume fraction of each phase is

$$\frac{\partial \alpha_q}{\partial t} + v_j \frac{\partial \alpha_q}{x_j} = 0 \quad (21)$$

Commercial programs, such as ANSYS-FLUENT, dealwith a number of methods for the spatial discretization of Eq. (19), which can be chosen by the operator, depending on the time variable discretization method (the explicit and implicit methods).
In the present work the high Resolution Interface Capturing (modified HRIC) implicit method is implemented[23], cited by [7].

E. Mathematical Formulation

Table 1 shows the parameters of the modeled combined SEN and mold configuration, as well as the physical properties of the steel and inclusions used in this work.
Fig.1.depict a combined SEN and mold, in which, liquid steel flows due to gravity (by the pressure difference between the liquid levels of the tundish and the mold top free surfaces.) from a holding tundish down through a submerged entry nozzle to continuous casting mold cavity. As described by [3] here, the steel freezes against the water-cooled copper walls to form a thin solid shell, which is continuously withdrawn from the bottom of the mold at a "casting speed" that matches the flow of the incoming metal [3]. In the present study, a bifurcated-ported submerged entry nozzle (SEN) is considered having horizontal outlet ports.The submergence depth of the SEN in the domain is 300 mm. The transport equations for thecombined SEN and moldwere computed for both as one domain [2].
Due to the physical properties of steel in a continuous casting machine (table 1) and the magnitude of theLiquid velocity involved, the fluid flow in this process is essentially in turbulent regime. For example, in continuous casting of a slab with a width of 1.3 m**,** thickness of 0.25 mand casting speed of 0.02 m/s, the Reynolds number in the nozzle zone with 0.06 mx0.08mcross-section becomes greater than 50000.

F.CFD options and assumptions

The three-dimensional flow was assumed to be steady and incompressible. Any entrainment of gases was neglected. Inclusions were assumed to be spherical with diameter 50 and 225 μm and density 5000 kg/m^3. Operating conditions were specified as being standard atmospheric pressure (101.3 kPa) and temperature of 20 ºC. Gravity was switched on at 9.81 m/s2, which will of course have a buoyancy influence on the hotter emerging jet.

The turbulence model chosen for 3D CFD modeling is the k-ω turbulence model of Wilcox [14] [5]. The Standard k-ω turbulence model predicts high shear flows and especially jet flow very accurately for 3D models as well. The standard near-wall function was selected for this model (to predict flow accurately close to walls, by modeling turbulent boundary layers). More complex phenomena like solidification and oscillating mold were not modeled.

G.Boundary conditions

The typical boundary conditions specified in the CFD combined model are shown in Figure1 above (as arranged in GAMBT). The 2D boundary conditions are similar to that of the 3D model.

Table 1 combined SEN and mold model parameters [2].

Model parameters	**Values**
Nozzle port size/Inlet port size (z×y) (m)	0.065×0.080
Nozzle angle	15^{o}
Submergence depth (m)	0.30
Mold/Domain geometry specification	Open bottom
Mold/Domain height (m)	2.55
Mold/Domain width (m)	1.3
Mold/Domain thickness (m)	0.25
Average inlet flow rate (m3/s)	0.00325
Casting speed (m/s)	0.02
Fluid density (kg/m3)	7020
Fluid dynamic viscosity (m2/s)	0.007
Particle size (diameter) ($(m\times10^{-6})$)	50, 225
Particle density (kg/m3)	5000
Turbulence model	*k-ω and realizable*
Inclusion motion model	Random walk, 1098 inclusion injected every diameter

Mold walls:

The walls will be considered to be adiabatic and stationary. However, the model can easily be altered to move the walls at casting speed and with a liquidus temperature imposed, to more closely simulate plant conditions for later optimization evaluations [24].

Narrow face wall:

The flow was modeled up to, but not including, the mushy zone forming the inside of the steel shell solidifying against the narrow face mold wall. To account for building of the solid shell against the mold wall, the narrow face computational boundary can be tapered inward with distance down the mold wall. As reported from [24] the model results were insensitive to the exact value of this small change in the size of the domain.

Bottom outlet

Trial and error methods have proven that the use of an atmospheric pressure outletresults in more physically correct solutions, than using an outflow (zero gradientoutlets).A pressure outlet was considered for this modeling, in which, normal gradients of all variables (including velocity, K, andε) were left at zero along the bottom outlet surface of the computational model domain.

Inlet boundary condition

The velocity inlet, specified as perpendicular to the inlet boundary. The velocity at the inlet gate was

taken as 1.29 m/s with the turbulence intensity of 5%.
All variables were assumed to have constant value at the inlet of the nozzle.

$v = v_{in}$, $u = w = 0$, $k = 001 v_{in}^2$, $\varepsilon = C_\mu \frac{k_{in}^{\frac{3}{2}}}{0.05D}$ (10)

It's noted that the value of k and ε were selected from semi-empirical equations presented [12].

Free surface:

The normal gradient of all variables were set to zero except the velocity perpendicular to the surface which itself was assumed zero

Symmetry faces:
The assumption of symmetry in the width of the mould allows one to only model half of the SEN and mould (2D &3D model). The solution is thus assumed to be identical in the two halves. By defining a symmetry planes, FLUENT can solve the entire mould model – by only solving a half model.
For transient VOF calculations under ANSYS Fluent, the k-ε Realizable turbulence model with Standard Wall Functions is used to capture the flow turbulence. Inlet
condition was: turbulent kinetic energy 0.008723 m^2/s^2, turbulent dissipation rate 0.02089 m^2/s^3[7]
For the purpose of the numerical simulations (VOF), the following properties of steel, slag and air were assumed, which are summarized in table2 [7]

Table 2 Properties of liquid steel, slag and air [7].

Properties/material	Steel	Slag	Air	Unit
Density (ρ)	7010	2600	1.225	kg/m^3
Viscosity (μ)	0.007	0.4	$1.789\ e^{-5}$	kg/m·s
Surface tension (σ)	slag/steel steel/air slag/air		1.6 0.007 0.007	N/m

IV. Computer characteristics

The computer used of this work has the following characteristics:

Table 3 computer characteristics

CPU	Intel ® Core ™ i3 CPU M330 @ 2.13 GHz
Memory	4 GB of RAM
Mass storage service	500 GB
Operating System	Microsoft Windows 7 64 bits

V. Solution Procedure

A. Initialization:

During the iteration process, certain milestones must be reached before switching to more accurate solver algorithms. For example, before the iteration process can commence, an initial solution must be guessed. This initial estimate of a flow field can thus be seen as a first milestone before the iteration process can begin [24].

B. Under- and over-relaxation factors:

It is often necessary to adjust the over-relaxation factors to prevent the non-linear Navier- Stokes equations from diverging. Under-relaxation comprises the slowing down of changes from iteration to iteration. Over-relaxation (accelerating these changes) is often used to test whether a "converged" solution is indeed converged and stable. By some trialsaexceptional steps have been developed by [27] to guarantee convergence of SEN and mould CFD problems. As soon as the solution seems to be nearing convergence, the relaxation factors can be adjusted upwards (towards over-relaxation) to ensure a true converged solution [27].

C. Wall functions – grid adaption necessary:

In order for the wall function to predict the near-wall flow correctly, the grid cells adjacent to the wall need to be sized correctly. The size is determined by the y+-value of that cell: the y+-value of a cell is a function of the velocity of and the properties (density, viscosity inter alia) of the fluid in that cell, and is in fact a local Reynolds number based on the friction velocity and the normal spacing of the first cell. For the k-ε and k-ω turbulence models, the wall function approach requires the y+-value to be between 50 and 500 [dimensionless] [27].

D. Mass imbalance regulation in the model

Whenever reverse flow is experienced over any boundaries in a CFD model, the situation may arise that mass imbalances occur. The SEN and mould CFD model is an example where mass imbalances

occur: due to a recirculation zone in the mould, reverse flow is experienced over the pressure outlet boundary[25]. These mass imbalances must be periodically rectified during the solution procedure using grid adaption (refer to the solution procedure section (G) below).

E. Summary of Boundary conditions:

o Casting speed: inlet SEN velocity scaled to exactly match flow rate of 0.0065 m^3/s
o Meniscus: zero shear stress wall
o Mould walls: adiabatic (by default) and stationary
o Outlet at atmospheric pressure.

o Material properties: Steel 7020 kg/m^3

G.The solution method or procedure comprises: First-order solution

To get quick convergence of the model of the combined SEN and mold the following steps were followed:

1- adapt (refine) grid for y+ values at walls and mass-imbalance
2- adjust under-relaxation forPressure correction equation and momentum equation as well as turbulence kinetic energy equation

The above steps should be repeated until convergence for first-order solution attended, and then the same steps repeated, when settings to second-order [27].

VI. Results and Discussion

The casting speed and the physical properties of the steel used in this simulation are given in Table 1. All results discussed below are for a 0.3 m submergence depth (which is defined as the vertical distance nom the meniscus to the center of the outlet ports of the nozzle) of the nozzle.
Trial and error methods proved that the choice of a turbulence model has a radical effect on this particular flow field. The flow field is sensitive to the combination of turbulence model; mesh quality and solution procedure followed. However, since the addition of the k-ω turbulence model to FLUENT in 2003 [12], this 2-equation model proved to be well suited for jet-like flows. The Standard k-ω model is based on the Wilcox k-ω model [14]. Both k-ω turbulence models (Standard (STD) and Shear Stress Transport (SST)) [22] incorporate modifications for low Re-number effects, compressibility, and shear flow spreading. Wilcox's model predicts shear flow spreading rates that are in close agreement with measurements for far wakes, mixing layers, as well as plane, round and radial jets. These models are thus applicable to wall-bounded flows and free shear flows.

In this work standard k-ε and Standard k-ω were used, but the Standard k-ω model proved to be most suited for 3D CFD models of the SEN and mould.

On the other hand, 2D modeling proved to be accurate with the k-ε Realizable model[25]. Although this model also assumes isotropic turbulence, the effect on the mean flow is negligible in 2D modeling. The k-ε Realizable model (as opposed to the Standard k-ε model) is more suited for flow features that include strong streamline curvature, vortices, rotation and complex secondary flow features [25]. The 2D modeling was used to track the slag and steel interface, to predict the slag entrapment in the steel melt, that because the 2D less time consuming than the 3D modeling.

Simulation runs were carried out for a casting speed of 0.02 m/s. Figures 4b and 4c show the predicted velocity fields, for the centrally symmetric vertical plane parallel to the wide face of the caster for 3D and 2D respectively.
As seen from the velocity fields displayed in these figures, the molten steel, supplied through the submerged entry nozzle, impinges onto the narrow face of the moldthen flow is separated into two oppositely directed streams, each of which moves parallel to the narrow face and later arranges a large recirculation zone. The upper recirculation flow is restrained by the meniscus surface and the wide face of the slab. The lower recirculation flow moves both downstream and towards the wide face of the slab and a portion of it returns towards the submerged entry nozzle. The flow field in the caster thus can be categorized by the location of the centers of the upper and lower recirculation zones and the impingement point. The two turbulent recirculation zones lead to the improvement of the mass, momentum and energy transport in the upper region of the mould[24].

A.Fluid flow pattern

Figures 4a, 4b, 4c, 4d and 4e compares the flow patterns predicted, in this work and from [2], [24][5] 18]for a typical double-roll flow pattern condition. In this particular flow pattern, the steel jets first impinge on the narrow faces before turning upward towards the top surface and back across towards the SEN as explained in VI above. And this was indicated in (Figure 4e) by PIV measurement/ time averaged velocity vectors field (center plane between wide faces) for flow in the mold cavity [5],

The flow pattern of this model (3D model) showed similar results as from [2]the only difference as can be seen from the diagrams(below) is that, the flow-out jet from SEN port is steeper down ward in the model of [2] fig. 4a, than of this work fig. 4b, that because the combination of the two devices in this work, led the flow through the SEN to impact firstly against the well of the SEN and then flowed out of the port of the SEN in the cavity of the mould, but the 2D model showed steeper flow jet fig. 4c. While from [24] fig. 4d, whowas initialized the flow from the SEN inlet, the flow pattern of this model showed typical results as from [24], who used also horizontal SEN outlet ports with the same casting speed of this work (0.02 m/s) and combined SEN and mold domain.

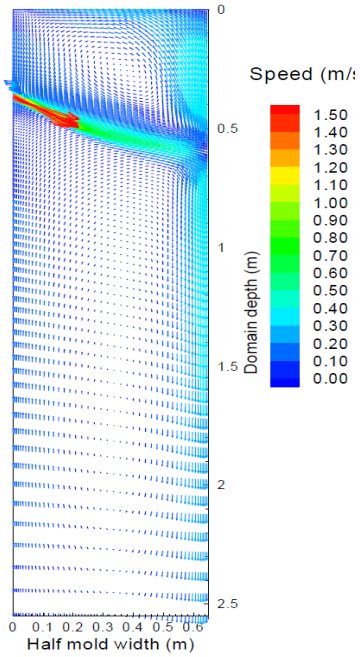

Fig. 4aComputed velocity vectors field at the vertical centrally symmetric plane paralleled to the wide facefor a casting speed of 0.02 m/sec initialised from mold inletwith horizontal SEN outlet port [2]

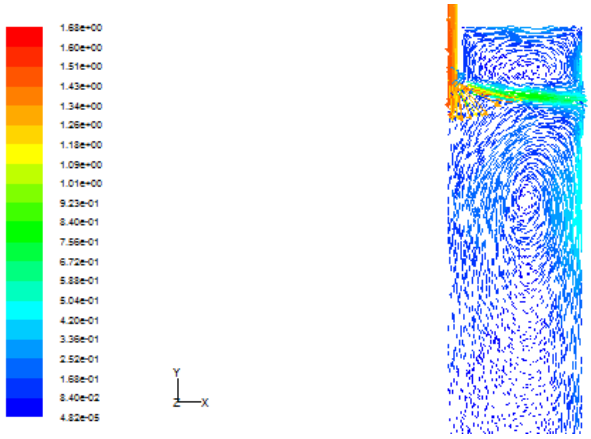

Fig. 4bthe present computed velocity vectors field at the vertical centrally symmetric plane paralleled to the wide face for a casting speed of 0.02 m/sec for 3D combined SEN and mold with horizontal SEN outlet port .

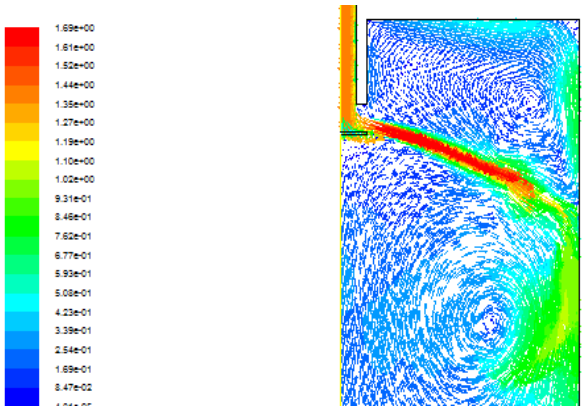

Fig. 4c the present2D CFD-model Computed velocity vectorsfield

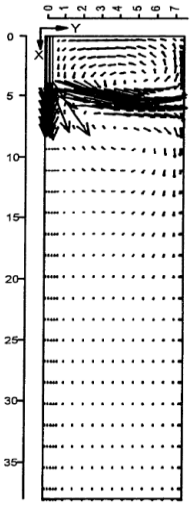

Fig. 4dComputed velocity vectors field at the vertical centrally symmetric plane paralleled to the wide face for a casting speed of 0.02 m/sec for combined SEN and mold with horizontal SEN outlet port[24].

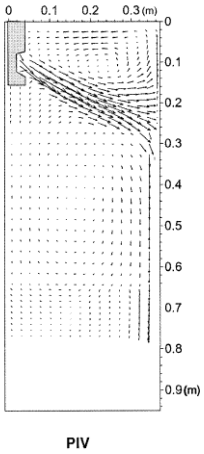

Fig. 4ePIV (using particle image velocimetry) measurement/time averaged velocity vectors field (center plane between wide faces) for flow in the mold cavity[5]

B.CFD model: Verification Results

1. Flow pattern

The first step to validate the model is to concentrate on the flow patterns only (momentum only), by exactly imitating the model from Thomas [2](see figures 4a-e). If the CFD momentum model closely matches the flow patterns of the model from[2], [5] [24], the model can be assumed to be acceptable, this was discussed in section (VI-A) above.

From here, it is rather a straightforward exercise to extend the model to imitate real plant circumstances, by scaling the geometry to the targeted plant, enabling the energy equation (and therefore allow temperature and buoyancy effects), and adjusting and supplementing the boundary conditions.

2. Inclusions removal

For the calculation of inclusion removal [2]has reported that, the calculation suggests that around 12% of the inclusions leaving the tundish stick to the SEN walls (removed by clogging). [2]explained with diagrams, that a uniform buildup on the nozzle walls, with increased tendency towards buildup on the SEN bottom due to impact from the flowing jet, and reported, that is consistent with observations of nozzle clogging where local reoxidation or chemical interaction were not the cause.They compared inclusion fractions entrapped at different destinations with the industrial measurements. For inclusions smaller than 50 µm entering the mold, only 7% are safely removed by the top surface, independent of inclusion size. A larger fraction of inclusions bigger than 50 µm are removed. The same authors modeledremoval of 50 µm and 225 µm and they reported that, only7-12% of the inclusions entering the mold are predicted to be removed by the top surface. Adding 12% sticking to the SEN walls as clogged material, the simulated inclusion removal from tundish to slab is 19-24%, which agrees well with their measurement of 22%.

In this work the removal of 50 µm and 225 µm were modeled, it was found that about 6-13% of the inclusions entering the mold are predicted to be removed by the top surface by adding 12% we got 18-25%, which is agree well the results from [3]. The small difference, when comparing the results, may be due to the difference of the nozzle outlet port angle, which is influence the flow jet from the nozzle into the mold cavity, which is steeper by them than by this work.

3.Slag-steel melt interface tracking by VOF method

The cause of slag entrapment can be seen in the low stability of shearing stresses occurring at the interface. This mechanism is explained in detail by the Kelvin – Helmholtz theory[26]. For explaining this phenomenon, studies[7] [26], on water models with the addition of different silicone oils,presents in Fig. 5 representing the Authors' ideas of the form of the slag–steel system interface.

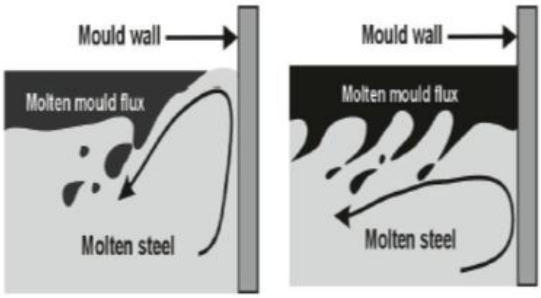

Fig. 5 Illustration of the slag entrapment phenomenon for two cases: with partially exposed steel surface (stationary conditions) – (a) and with no exposed metal surface (non-stationary conditions) – (b) [7][26].

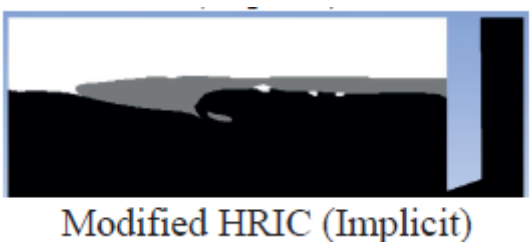

Fig. 6 Illustration of the slag entrapment[7]

The view image in Fig. 6 is very similar to the results of the present simulation (Fig. 7c), in which the Modified HRIC (Implicit) procedure is used. [7] Has used different discretization schemes of the interface tracking and got similar result to the

illustration in fig. by using the Modified HRIC (Implicit) procedure.

The formation of interfaces on the examined object's section was observed within the entire period of time, from the moment of starting filling the mold with steel until the stabilization of steel and slag motion. Figure 6a -d shows the direct region of liquid slag interaction with the surface of steel in the mold, at the second 4,10, 20, 34 and … respectively, of process duration, as computed using the Modified HRIC (Implicit) numerical procedures.

In the region at the side mould wall the steel surface is elevated compared to the initial state. This is caused by the circulatory motion of the upper vortex (see Fig. 7a,b).

Based on the results of study [28] cited by [4] it has been found that for the phenomenon of slag entrainment by the metal bath to occur, the velocity of liquid steel motion in the sub-meniscus zone must exceed the value of 0.2 m/s. In the mold configuration used in this study,the maximum velocity of liquid steel motion below the meniscus level was 0.4 m/s (at second 34) as illustrated in fig 8, which indicate powder entrapment and indirectly confirmed the finding due to the slag contours indicated in fig. 7d (at second 34)

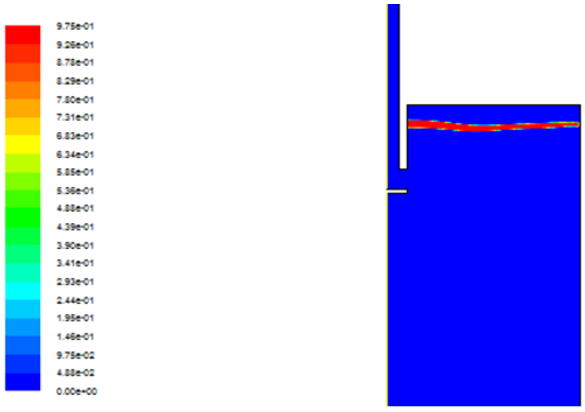

Fig. 7a the picture of the liquid steel and slag interaction state modeled by the VOF method (FLUENT) after a time of 4s

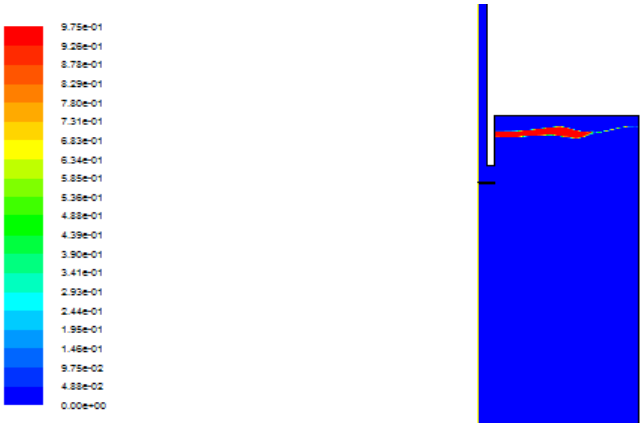

Fig. 7bthe picture of the liquid steel and slag interaction state modeled by the VOF method (FLUENT) after a time of 10s

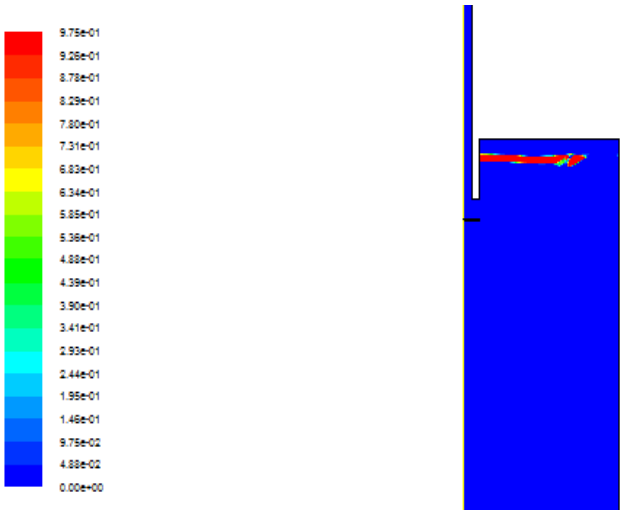

Fig. 7cthe picture of the liquid steel and slag interaction state modeled by the VOF method (FLUENT) after a time of 20 s

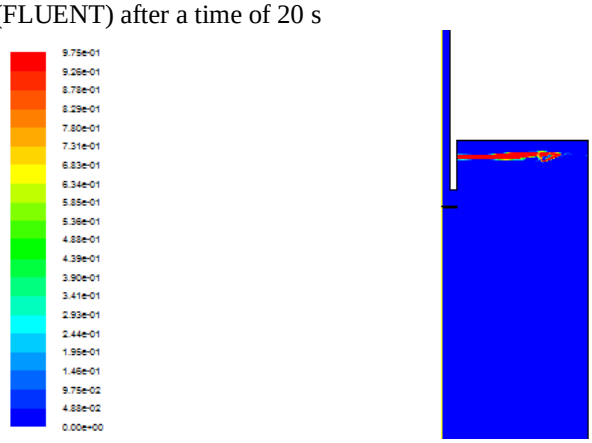

Fig. 7d the picture of the liquid steel and slag interaction state modeled by the VOF method (FLUENT) after a time of 34 s

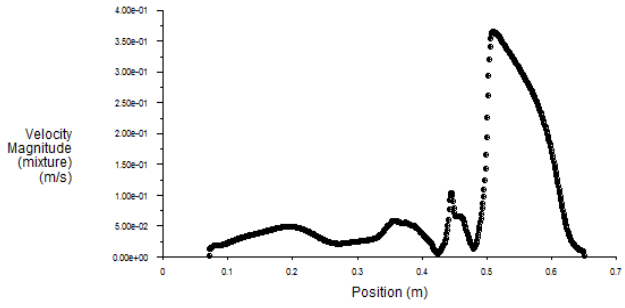

Fig. 8 Values of liquid steel velocity along the horizontal line located at the interface of steel slag below meniscus level at 34s

VI. Conclusion

In the present study**,** a three-dimensional control volume based finite-difference model was implemented, by using CFD code (FLUENT).A3D k - ***ω***model was used to account for the turbulence effects in the liquid metal as well asa 2D model k-ε Realisable model. Numericalaccuracy of the model was tested by comparing it to the model results and plant measurement from [2] [3]

A discrete face model of particle transport during continuous casting of steel slabs were performed, based on steady flow velocity fields obtained from k-ω simulations of the three-dimensional fluid flow mentioned above. The particles entered the mold cavity considered to be entrapped to the narrow and wide walls and escaped through the outlet and removed at the top surface, the results was compared and validated with results and plant measurement from [2] [3].

The higher removal for larger particles was mainly due to their smaller chance of capture, in addition to their larger buoyancy.

The present study clearly signified the importance and need for a three-dimensional CFD modeling to optimize the process of the continuous casting mold. Also due to small fraction of the inclusions removed to the top slag of the mold, inclusions should be removed in the prior vessels of the process ie. the ladle and the tundish.

In the present study, the multiphase VOF model was used, which allows the differences in the liquid slag level to be determined during the continuous steel casting process.

Application of the time discretization procedure following the Implicit scheme (Modified HRIC) was used, because it require shorter time than explicit scheme as reported by [7], who was tested many discretization procedures. This discretization scheme examines the interface behaviour of the mould powder originating liquid slag in the mould during continuous steel casting. The aim was to explain the mechanisms of slag entrapment and to reduce this phenomenon during steel casting.

The recorded variations in slag layer height were differed, depending on the location of the monitoring point. The highest liquid slag level was observed near the narrower mold wall, while the lowest – in the vicinity of SEN.

The tracked interfaces of the steel–slag–air system by using the VOF method enable one to assess the degree of liquid slag entrapment into steel due to the occurrence of instability of shearing stresses at the interface, as explained by the Kelvin - Helmholtz theory. Thepictures in (fig.7a-d),indicate slag entrapment for the configuration used in this study.

Future Work

The first step would be to eliminate the isothermal assumption employed in the current study by including heat losses from the mold and thereby also the buoyancy driven flows present in the industrial continuous casting mold and predicting surface turbulence effects. Also the influence of the change of the out port angle of the SEN in the continuous casting mold cavity should be examined to assess, its influence on the slag entrapment in the steel melt .

The mold walls should be altered to move at casting speed and with a liquidus temperature imposed, to more closely simulate plant conditions for later optimization evaluations.

References:

[1] H. K. Versteeg and W. Malalasekera, An Introduction to Computational Fluid Dynamics (The finite Volume Method), *Harlow: Pearson Education Limited,Second edition published , pp. 1-517 , 2007.*

[2] B. G. Thomas. Lifeng Zhang (Dr.), "Fluid Flow and Inculsion Motioninthe Continuous Casting Strand," *in XXIV Steelmaking National Symposium, Morelia, Mich, Mexico,pp. 184-196, 26-28, Nov.2003.*

[3] B. G. Thomas, Q. Yuan, L. Zhang and S. P. Vanka, "Flow Dynamics and Inclusion Transport in Continuous Casting of Steel," *in 2003 NSF Design, Service, and Manufacturing Grantees and Research Conf., Jan. 6-9 (2003).*

[4] M. Bilenicki, J Jowsa and A. Cwudzinski, Multiphase numerical Model of Molten Steel and Slag behavior in the Continuous Casting Mould, *Archives of Metallurgy and Materials, Volume 60, 2015, Issue 1, 257-262..*

[5] B. G. Thomas, Q. Yuan and S. Sivaramakrishn, "Comparison of Four Methods to Evaluate Fluid Velocities in a Continuous Slab Casting Mold," *ISIJ International, pp. 1262–1271, Vol. 41, No. 10 (2001),.*

[6] Huang, X., & Thomas, B. G. Intermixing model of continuous casting during a grade transition. *Metallurgical and Materials Transactions B, 27(4), 617-632.1996.*

[7] J. Jowsa, M. Bielnicki and A. Cwudziński, "Numerical modelling of metal/flux interface in a continuous casting mould," *Archives of Metallurgy and Materials, Volume 60(4), 2905-2912. 2015.*

[8] S. Liu , M. Liang, S. Niu and C. Li, "Unsteady State and Inclusion Control during Steel Continuous Casting," *AIS Tech., 2006 Proceedings - Volume 1. PP. 915*

[9] Q. Lu, R. Yang, X. Wang, J. Zhang and W. Wang, "Water modeling of mold powder entrapment in slab continuous casting mold. *Journal of University of Science and Technology Beijing, Mineral, Metallurgy, Material, 14(5), pp.399-404. 2007.*

[10]] L. C. Hibbeler, R. Liu and B. G. Thomas, "Review of Mold Flux Entrainment Mechanisms and Model Investigation of Entrainment by Shear-Layer Instability," *in Control of solidification structures and management of defects, Session 12, Düsseldorf, 27 June – 1 July 2011.*

[11] S. M. CHO, S. KIM and B. G. THOMAS, "Transient Fluid Flow during Steady Continuous Casting of Steel Slabs: Part I. Measurements and Modeling of Two-phase Flow," *ISIJ International, pp. 845–854, Vol. 54 (2014), No.4.*

[12] "Guide, Fluent User'S. "Ve rsion 6.3, *Fluent." Inc, Lebanon (2006).*

[13] S. Sivaramakrishnan, B. G. Thomas and S. P. Vanka, "Large Eddy Simulation of Turbulent Flow in Continuous Casting of Steel," *Materials Processing in the Computer Age, 3, pp.189-198. 2000.*

[14] Wilcox, D. C. Turbulence modeling for CFD *(Vol. 2, pp. 103-217). La Canada, CA: DCW industries, 1998.*

[15] Yuan, Q., Zhao, B., Vanka, S. P., & Thomas, B. G. Study of Computational Issues in Simulation of Transient Flow in Continuous Casting. *steel research international, 76(1), 33-43, 2005.*

[16] Q. Yuan, T. Shi, S. P. Vanka and B. G. Thomas, "Simulation of Turbulent Flow and Particle Transport in the Continuous casting of Steel," The Mater., Minerals, & Metals Soc., Warrendale, PA, pp. 491-500, 2001.

[17] O. J. ILEGBUSI and J. SZEKEL, "Interfacial Phenomena and Computational Fluid Mechanics in materials, Processing," *,ISIJ International, pp. 943-950, Vol. 34 (1 994), No,12.*

[18] B. G. THOMAS and L. ZHANG, "Mathematical Modeling of Fluid Flow in Continuous Casting," *ISIJ Internationa, pp. 1181–1193, Vol. 41, No. 10, (2001)*

[19] L. Zhang, J. Aoki and B. G. Thomas, "Inclusion Removal by Bubble Flotation in Continuous Casting Mold," *Metallurgical and materials transactions b, 37(3), 361-379, 2006.*

[20] L. Zhang and B. G. Thomas, "Application of computational Fluid Dynamics to Steel Refining and Casting," *in Fourth International Conference on CFD in the Oil and Gas,Metallurgical & Process Industries, SINTEF / NTNU, Trondheim,pp. 1-9 Norway, 6-8 June 2005.*

[21] Y. Wang and L. Zhang, "Transient Fluid Flow Phenomena during Continuous Casting: Part II—Cast Speed Change, Temperature Fluctuation, and Steel Grade Mixing," *ISIJ International, pp. 1783–1791, Vol. 50 , No. 12,2010*

[22] F. R. MENTER , "2-Equation Eddy-viscosity Turbulence Models for Engineering Application," *AIAA Journal, p. pp. 1598 – 160, Vol. 32, No. 8, 1994.*

[23] S. Muzaferija, M. Peric, P. Sames and T. Schelin, "A two-fluid Navier-Stokes solver to simulate water entry," *in Proc. Twenty-Second Symposium on Naval Hydrodynamics., (1988).*

[24] Seyedein, S. H. "Three-dimensional modeling of various slab and thin-strip twin-roll casting processes." *(2000): 45-87.*

[25] G.J acobus de Wet, "CFD Modeling and Mathematical Optimization of Continuous Caster Submerged Entry nozzle, " *Master of Engineering (Mechanical)/Department of Mechanical and aeronauical Engineering/ University of Pretoria, 2007.*

[26] M. Iguchi, J. Yoshida, T. Shimizu and Y. Mizuno, "Model Study on the Entrapment of Mold Powder into Molten Steel," *ISIJ International, pp. 685-691, Vol.40, (2000).*

[27] De Wet, G. J. (2005): M. E. *Thesis University of Pretoria.*

[28] introduction to continuous casting http://ccc.illinois.edu/itroduction.htm

[29] A. Prabhaka, CFD Analysis of Static Pressure and Dynamic Pressure for NACA 4412 , *International Journal of Engineering Trends and Technology (IJETT) - Volume4 Issue8- August, Page 3258 2013*